

## Wavelet entropy of BOLD time series

**Citation for published version (APA):**

Gupta, L., Jansen, J. F. A., Hofman, P. A. M., Besseling, R. M. H., de Louw, A. J. A., Aldenkamp, A. P., & Backes, W. H. (2017). Wavelet entropy of BOLD time series: an application to Rolandic epilepsy. *Journal of Magnetic Resonance Imaging*, 46(6), 1728-1737. <https://doi.org/10.1002/jmri.25700>

**DOI:**

[10.1002/jmri.25700](https://doi.org/10.1002/jmri.25700)

**Document status and date:**

Published: 01/12/2017

**Document Version:**

Publisher's PDF, also known as Version of Record (includes final page, issue and volume numbers)

**Please check the document version of this publication:**

- A submitted manuscript is the version of the article upon submission and before peer-review. There can be important differences between the submitted version and the official published version of record. People interested in the research are advised to contact the author for the final version of the publication, or visit the DOI to the publisher's website.
- The final author version and the galley proof are versions of the publication after peer review.
- The final published version features the final layout of the paper including the volume, issue and page numbers.

[Link to publication](#)

**General rights**

Copyright and moral rights for the publications made accessible in the public portal are retained by the authors and/or other copyright owners and it is a condition of accessing publications that users recognise and abide by the legal requirements associated with these rights.

- Users may download and print one copy of any publication from the public portal for the purpose of private study or research.
- You may not further distribute the material or use it for any profit-making activity or commercial gain
- You may freely distribute the URL identifying the publication in the public portal.

If the publication is distributed under the terms of Article 25fa of the Dutch Copyright Act, indicated by the "Taverne" license above, please follow below link for the End User Agreement:

[www.tue.nl/taverne](http://www.tue.nl/taverne)

**Take down policy**

If you believe that this document breaches copyright please contact us at:

[openaccess@tue.nl](mailto:openaccess@tue.nl)

providing details and we will investigate your claim.

# Wavelet Entropy of BOLD Time Series: An Application to Rolandic Epilepsy

Lalit Gupta, MSc,<sup>1</sup> Jacobus F.A. Jansen, PhD,<sup>1,2</sup> Paul A.M. Hofman, PhD,<sup>1,2</sup>  
René M.H. Besseling, PhD,<sup>1,3</sup> Anton J.A. de Louw, PhD,<sup>3,4</sup>  
Albert P. Aldenkamp, PhD,<sup>2,3,4</sup> and Walter H Backes, PhD<sup>1,2\*</sup>

**Purpose:** To assess the wavelet entropy for the characterization of intrinsic aberrant temporal irregularities in the time series of resting-state blood-oxygen-level-dependent (BOLD) signal fluctuations. Further, to evaluate the temporal irregularities (disorder/order) on a voxel-by-voxel basis in the brains of children with Rolandic epilepsy.

**Materials and Methods:** The BOLD time series was decomposed using the discrete wavelet transform and the wavelet entropy was calculated. Using a model time series consisting of multiple harmonics and nonstationary components, the wavelet entropy was compared with Shannon and spectral (Fourier-based) entropy. As an application, the wavelet entropy in 22 children with Rolandic epilepsy was compared to 22 age-matched healthy controls. The images were obtained by performing resting-state functional magnetic resonance imaging (fMRI) using a 3T system, an 8-element receive-only head coil, and an echo planar imaging pulse sequence ( $T_2^*$ -weighted). The wavelet entropy was also compared to spectral entropy, regional homogeneity, and Shannon entropy.

**Results:** Wavelet entropy was found to identify the nonstationary components of the model time series. In Rolandic epilepsy patients, a significantly elevated wavelet entropy was observed relative to controls for the whole cerebrum ( $P=0.03$ ). Spectral entropy ( $P=0.41$ ), regional homogeneity ( $P=0.52$ ), and Shannon entropy ( $P=0.32$ ) did not reveal significant differences.

**Conclusion:** The wavelet entropy measure appeared more sensitive to detect abnormalities in cerebral fluctuations represented by nonstationary effects in the BOLD time series than more conventional measures. This effect was observed in the model time series as well as in Rolandic epilepsy. These observations suggest that the brains of children with Rolandic epilepsy exhibit stronger nonstationary temporal signal fluctuations than controls.

**Level of Evidence:** 2

**Technical Efficacy:** Stage 3

J. MAGN. RESON. IMAGING 2017;46:1728–1737.

Brain regions show spatial patterns of coherent blood-oxygen-level-dependent (BOLD) activity during resting-state functional magnetic resonance imaging (rsfMRI). Recent studies have indicated that, in addition to variations in spatial patterns, resting-state activity also shows complex nonstationary BOLD signal fluctuations in rsfMRI time series.<sup>1–3</sup> However, most of the contemporary methods for analysis of rsfMRI data are based on the detection of similarities between time series of different brain regions or on the correspondence of time series to a predefined model, but do not capture temporal irregularities in the signal. A method that merely compares the time signals of various brain regions will be insensitive to similar irregularities,

which could be critical for characterization of BOLD time series in certain diseases like epilepsy.<sup>4–6</sup> However, a method that characterizes the intrinsic aberrant irregular temporal aspects of time series signal in rsfMRI is currently lacking. Such a method should ideally be able to quantify the temporal disorder/order of brain fluctuations on a voxel-by-voxel basis.

The fluctuations of the BOLD time series are a combination of oscillations that are active in a complex manner in several frequency ranges. The spectral entropy can be used to quantify the disorder/order of these time series.<sup>7</sup> For instance, the spectral entropy would be low for a pure sinusoidal signal (one frequency, hence one peak) and high for a noise signal (all frequencies, hence wider spectrum). However, this method

View this article online at [wileyonlinelibrary.com](http://wileyonlinelibrary.com). DOI: 10.1002/jmri.25700

Received Dec 12, 2016, Accepted for publication Feb 24, 2017.

\*Address reprint requests to: W.H.B., Departments of Radiology and Nuclear Medicine, Maastricht University Medical Center (MUMC+), P.O. Box 5800, 6202 AZ Maastricht, the Netherlands. E-mail: [w.backes@mumc.nl](mailto:w.backes@mumc.nl)

From the <sup>1</sup>Departments of Radiology and Nuclear Medicine, Maastricht University Medical Center, Maastricht, Netherlands; <sup>2</sup>School for Mental Health & Neuroscience, Maastricht University Medical Center, Maastricht, Netherlands; <sup>3</sup>Department of Electrical Engineering, Eindhoven University of Technology, Eindhoven, Netherlands; and <sup>4</sup>Epilepsy Center Kempenhaeghe, Heeze, Netherlands

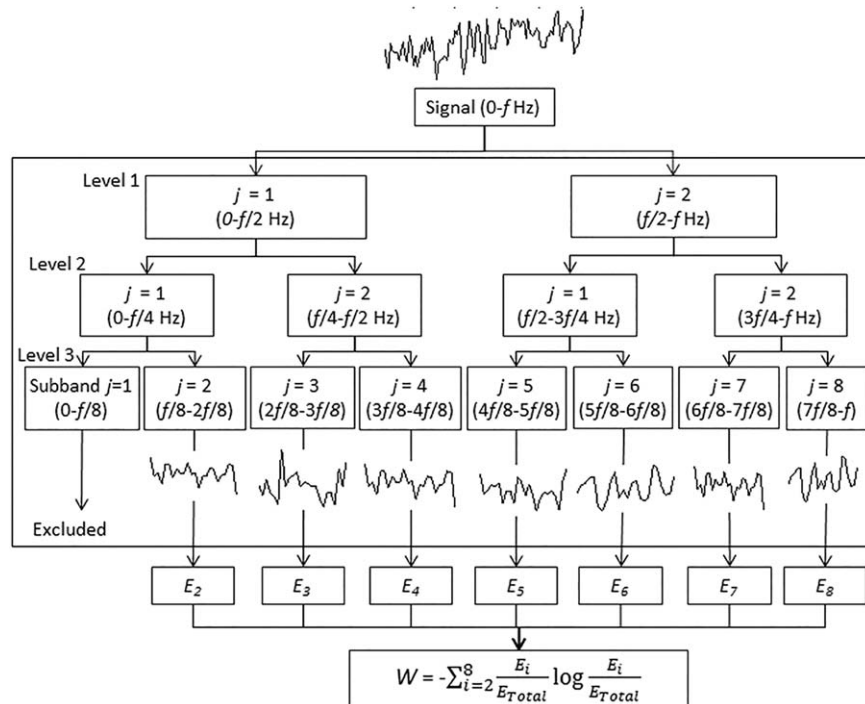


**FIGURE 1:** Block diagram illustrating the methodology for computing the wavelet entropy measure. The time series signal, sampled at frequency  $f$ , is decomposed down to three levels using the Daubechies full tree dyadic discrete wavelet transform. The wavelet entropy ( $W$ ) is calculated using the relative energy ( $E/E_T$ ) of each subband.

is less appropriate for BOLD time series, because the discrete Fourier transform (DFT) requires stationarity of the brain signal, which is likely nonstationary.<sup>8</sup> Short-time Fourier transform (STFT) uses DFT in small time-evolving windows, assuming signals as quasistationary within the sliding window, which resolves some of the shortcomings of DFT. However, due to the uncertainty principle, one critical limitation appears when windowing the data: if the window is too short (high temporal resolution), the frequency resolution will be poor, and if the window is too long (low temporal resolution), the time localization will be less precise. Furthermore, STFT is rather inconvenient for BOLD time series as the number of samples (and sample frequency) is often too limited in comparison to, for instance, electroencephalographic recordings.<sup>9</sup> An alternative approach to overcome these limitations, is to use a time-frequency representation of the time signal as provided by the wavelet transform. The orthogonal discrete wavelet transform (DWT) makes no assumptions about stationarity and analyzes the signal at different frequency subbands with different time resolutions.<sup>10</sup> With DWT, the time-frequency structure of the signal can be followed with optimal temporal resolution and the signal is represented as amplitudes (and energy) over various wavelet coefficients, by which the frequency subbands can be followed over time.<sup>11</sup> The wavelet entropy measure is computed over the wavelet subbands as the integral of the squared wavelet components over time and represents the disorder/order of the time signal.

The objective of this work was to study the use of the wavelet entropy measure to capture the cerebral fluctuations represented by nonstationary effects in the BOLD time series. For epilepsy in general, it is known that the brain may express abnormal dynamic fluctuations either as epileptiform or direct seizure activity.<sup>12,13</sup> Therefore, a further objective was to analyze the wavelet entropy measure in epilepsy, for which we set out a comparison study between children with Rolandic epilepsy and healthy controls.

## Materials and Methods

### Wavelet Entropy Method

The wavelet entropy method analyzes the changes in order/disorder of the signal over the wavelet subbands. First, the signal is decomposed using the full tree dyadic DWT.<sup>10</sup> Then the entropy over subbands is calculated.<sup>3,14,15</sup> A block diagram of the complete methodology is shown in Fig. 1.

**WAVELET TRANSFORM.** The Wavelet Transform is a method to analyze a signal within different frequency ranges by means of dilating and transiting of a single function termed mother wavelet.<sup>16</sup> The DWT is implemented by Mallat's algorithm.<sup>10,17</sup> The Mallat algorithm uses lowpass and highpass filters to divide the input signal into high and low frequency components, ie, the signal  $S_j$  over subbands indexed  $j$  (both approximate and detailed subbands). This process is repeated by applying the downsampled filter output into another identical filter pair. The process is repeated to obtain a set of approximation (lowpass signal) and a detail

(highpass signal) subbands ( $S_j$ ). In this study, full tree wavelet decomposition is used, which is depicted in Fig. 1.

In the present work, the Daubechies<sup>16</sup> wavelet is chosen as the mother wavelet function because the corresponding algorithm picks up minute details that can be missed by other wavelet algorithms, like the Haar wavelet algorithm. Even if the signal is not represented well by one member of the Daubechies family, it may still be efficiently represented by another.

**WAVELET ENTROPY.** Each time series was decomposed into different wavelet subbands using the Daubechies-4 wavelet full tree (up to three levels). The lowest wavelet coefficient, or subbands, ( $S_j$ ) (<31 mHz) was excluded from the analysis to avoid contamination of slow signal drifts. The method to calculate wavelet entropy is as follows:

Let  $S_j(k)$  represent the timepoint  $k$  of subband  $j$ . Energy  $E_j$  in subband  $j$  will be given as:

$$E_j = \sum_{k=1}^N S_j(k)^2$$

where  $N$  is the number of timepoints per subband. The total energy over all the subbands is then:

$$E_T = \sum_{j=2}^8 E_j$$

and the wavelet entropy,  $W$ , is computed as:

$$W = - \sum_{j=2}^8 p_j \log p_j$$

where  $p_j = \frac{E_j}{E_T}$ .

A complete random signal will have a wavelet representation with equal energy over all subbands (ie, a completely inhomogeneous signal). Hence, the wavelet entropy will be maximal. On the other hand, for a wavelet representation of a signal with a contribution to only one subband ( $j$ ), thus no distribution, the wavelet entropy will be zero (as  $E_j = E_T$  and  $\log(E_j/E_T) = 0$ ). However, a typical BOLD signal reflects a more homogeneous time series and a frequency structure in which the energy roughly decreases as a function of frequency (subband), due to the lowpass nature of the hemodynamic response. When the distribution of energies over frequency subbands becomes more equal (ie, more random, more equally distributed frequency structure due to abnormality), the wavelet entropy increases.

### Model Time Series

A model time series consisting of two harmonic components and nonstationary components (either a dampened sinusoidal wave or random noise signal) with varying amplitudes, and its wavelet subbands and Fourier spectrum, are shown in Fig. 2. Figure 3 illustrates the values of wavelet entropy for various types of dynamic signals.

### Subjects

The study was approved by the Ethical Review Board. The parents or guardians of all children gave written informed consent for study participation. At our specialized epilepsy referral center neurological examinations and electroencephalogram (EEG) recordings were obtained for all patients. Two pediatric neurologists independently

analyzed clinical and seizure characteristics to confirm the diagnosis of Rolandic epilepsy. To confirm the diagnosis, agreement between the pediatric neurologists and EEG confirmation was required.<sup>18</sup>

After confirmation, 22 children with Rolandic epilepsy (eight girls; age, mean  $\pm$  SD:  $11.3 \pm 2.0$  years) were selected for the study. A 24-hour EEG selection criteria included centrotemporal spikes on EEG and concordant seizures etiology representing anarthria, hemiconia involving the face and/or unilateral extremities, or secondarily generalized seizures. Rolandic spikes were in the centrotemporal region either in only one hemisphere or independently on both sides. In some of the patients, spikes were broad and tended to spread to the adjacent regions. Rolandic spikes were diphasic high-voltage (100–300  $\mu$ V) sharp waves with a transverse dipole; they were often followed by a slow wave. The EEG data were analyzed by two clinical neurophysiologists. In cases of poorly observed nocturnal seizures, post-ictal signs of generalized seizures or confirmation of post-ictal hemiparesis was sufficient for inclusion in case of otherwise typical EEG. Further details were previously described.<sup>18</sup> In addition, 22 healthy controls were enrolled in the study (11 girls, age  $10.5 \pm 1.6$  years). All patients had an IQ  $>70$  and all controls attended regular education, and had neither (a history of) neurological disorders, nor learning problems.

### MRI

Imaging was performed on a 3T MRI systems (Philips Achieva, Best, the Netherlands) using an 8-element receive-only head coil. Conventional structural MRI and resting-state fMRI was applied. Structural imaging included a  $T_1$ -weighted sequence. A 3D fast-spoiled gradient echo sequence was used, employing echo time / repetition time / inversion time (TE/TR/TI) 38/8300/1022 msec, a cubic voxel size of 1 mm, and an acquisition time of 8 minutes. The rsfMRI involved a task-free  $T_2^*$ -weighted BOLD sequence of  $N = 195$  dynamic image volumes at a TR of 2 seconds, resulting in an acquisition time of 6.5 minutes. Further settings included: EPI sequence, TE 35 msec, pixel size 2 mm, and 4-mm thick axial slices.

### Image Processing

The functional images were slice-time and motion-corrected and spatially coregistered to the Montreal Neurological Institute (MNI) anatomical scan. To correct for nonneurophysiological signal fluctuations, the mean time series signal of the white matter and ventricular cerebrospinal fluid were calculated by averaging the signal over all corresponding voxels. Mean white matter and cerebrospinal fluid time series were then used as time-dependent covariates to correct gray matter time series by linear regression.<sup>19,20</sup> Gray matter, white matter, and cerebrospinal fluid voxels were segmented from the  $T_1$ -weighted images (Freesurfer) to obtain the specific time series signals.<sup>21,22</sup> Functional MRI images were smoothed with an 8-mm (full-width-at-half-maximum) 3D Gaussian kernel (SPM8 software). Analysis was performed on the gray matter of the whole cerebrum. Additionally, the Rolandic strip was also separately analyzed since patients with Rolandic epilepsy are known to generate discharges in either left and/or right sensorimotor cortex.<sup>12</sup> The BOLD time series might be affected by artifacts due to head movement or high-duty gradient system switching, seen as time spikes in the time series. Multiple time spikes may be found across BOLD time series, which

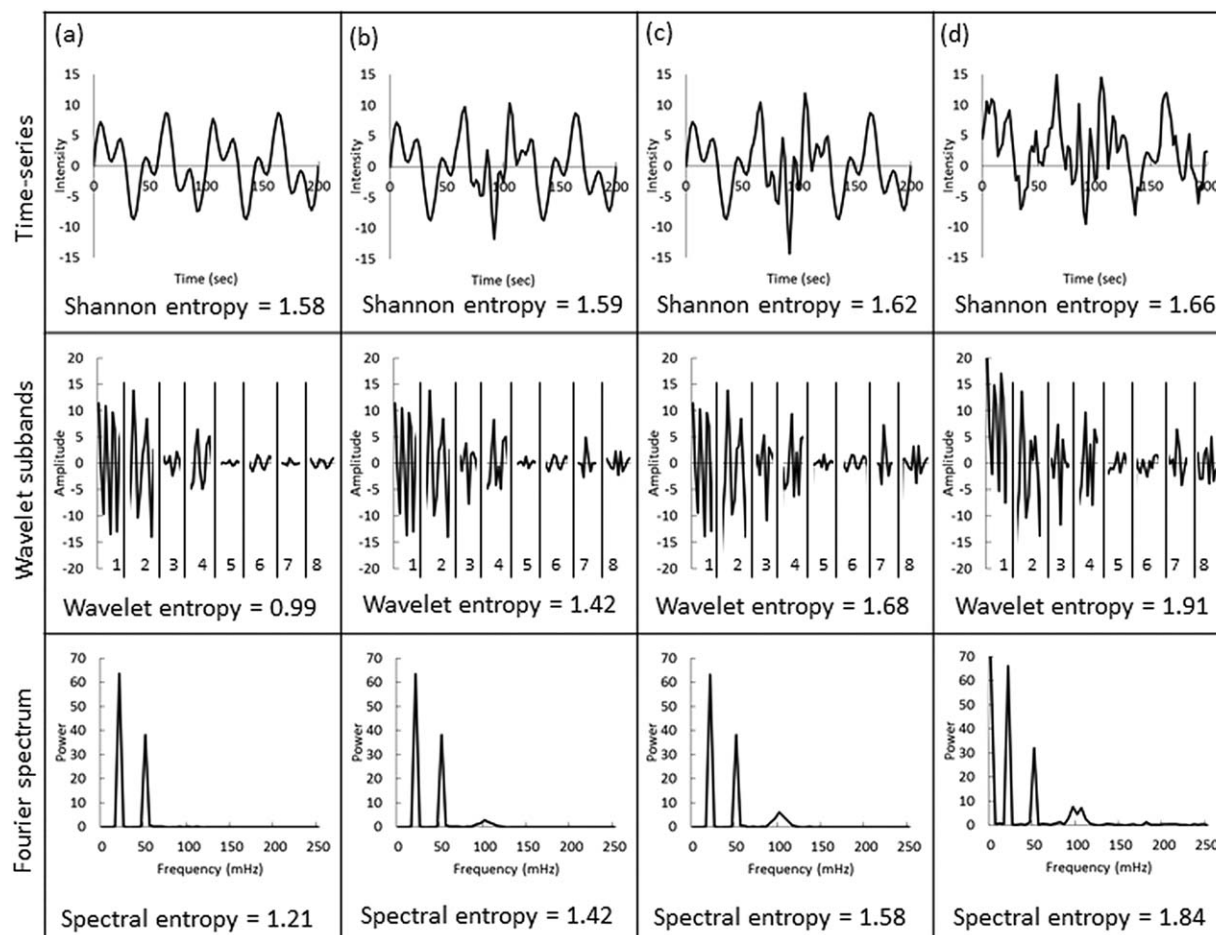


**FIGURE 2:** Model time series with two harmonic and one varying nonstationary component, the pertaining wavelet subbands and Fourier spectrum. (a) Time series signal with two time shifted sine waves, (b) a nonstationary wave (dampened sine curve) added to (a), (c) a nonstationary wave with higher amplitude added to (a), and (d) white noise added to (c). Wavelet subbands show relatively strong frequency components related to the two sine waves in certain subbands. The nonstationary components appear in subbands 3, 7, and 8, and their amplitudes increase from (b–c). The wavelet entropy increases relatively more than the Shannon entropy or spectral entropy from (a–d).

if not removed, may bias the wavelet entropy measure. Therefore, time spikes were removed from all the time series using time spike removal algorithm by Patel et al.<sup>23</sup> Figure 4 shows an example time series from a patient before and after time spikes removal. For statistical parametric mapping purposes, images were spatially normalized to the MNI standard space (SPM software, v. 8; Wellcome Department, University College London, UK). Wavelet entropy maps were created and superimposed on to the anatomical images to depict the distribution over the whole brain.

### Alternative Disorder/Order Measures

To assess the effectiveness, the results of the wavelet entropy measure were compared with other time series measures that characterize temporal characteristics of disorder/order as outlined in Table 1.

Spectral entropy measures have previously been used in the literature for EEG signals. To compute the spectral entropy, first a Fourier transform was applied to determine the power spectrum of the time series from which the spectral entropy as a measure of order/disorder<sup>8,24</sup> was calculated. Regional homogeneity (ReHo) is a measure of spatiotemporal homogeneity, and is often used in studies on temporal lobe epilepsy.<sup>25–28</sup> Basically, for the ReHo method Kendall's coefficient of concordance between the time series

of each voxel and its multiple neighboring voxels is calculated. The Hurst exponent is a measure of long-term memory, or measure of fractality of the BOLD signal.<sup>29</sup> To our knowledge, the Hurst exponent and spectral entropy measures have thus far not been described in the literature on epilepsy and BOLD signals.

Additionally, the Shannon entropy of the complete time series was also calculated for comparison.

Also measures, which are not used to measure order/disorder of BOLD time series such as the fractional amplitude in low frequency fluctuations (fALFF) and the wavelet energy were calculated. To compare the spectral entropy with the wavelet entropy at the subband intervals, the spectral energy was calculated also for the subband frequency ranges. For this, the spectral energy was averaged over the seven different frequency subbands.

### Statistical Analysis

Student's *t*-test was used for statistical assessment of any potential differences between patients with Rolandic epilepsy and healthy controls. Analyses were performed for each voxel and the results were obtained for the entire cerebrum and Rolandic strip. For the wavelet entropy measure, the diagnostic classification between

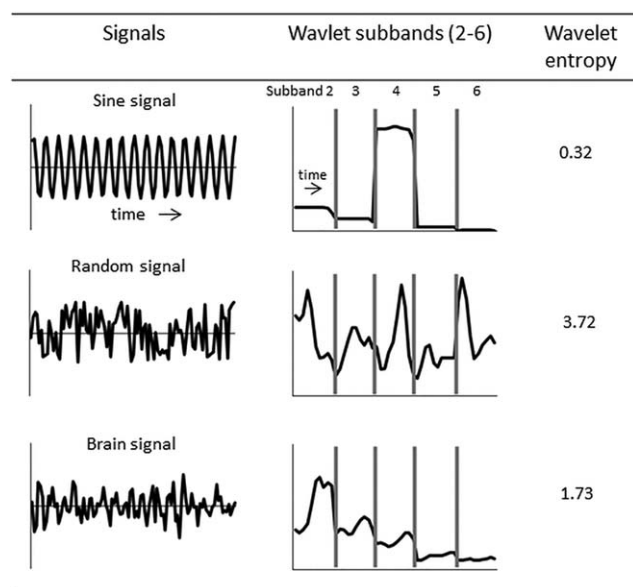


FIGURE 3: Comparison of the wavelet entropy measure computed from a (stationary) sine wave, a completely random signal, and a mean gray matter signal of a healthy control subject. Wavelet subbands represent the information distribution in different subbands (2–6) of a signal. For a random signal the information is more or less equally distributed over all subbands, whereas for a sine signal the information distribution is predominantly limited to only one subband. Therefore, the wavelet entropy is higher for the random signal and lower for the sine signal. For the brain signal, the information distribution gradually decreases from lower to higher subbands. Therefore, the brain wavelet entropy is in between that of the sine and random signal.

patients and controls was performed using support vector machine with a linear kernel<sup>30</sup> and 10-fold cross-validation. Sensitivity and specificity were computed for the entire cerebrum. The area under the receiver operating characteristic (ROC) curve was also computed.  $P < 0.05$  was considered statistically significant.

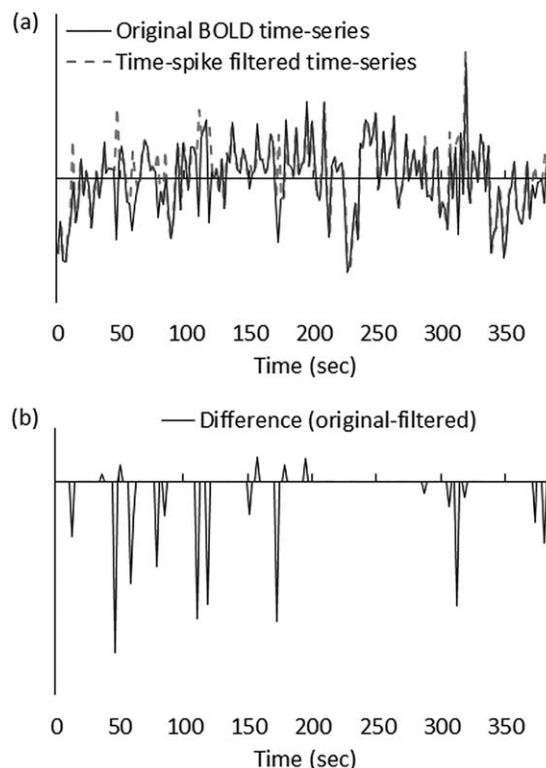
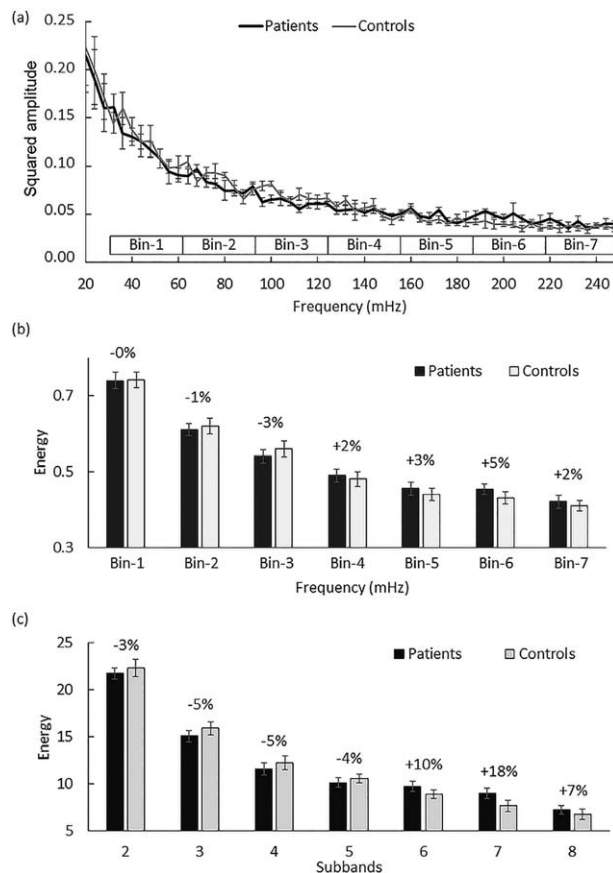


FIGURE 4: Illustration of the time spike removal algorithm applied to a BOLD time series signal of a patient. In (a) an example BOLD time series signal is depicted before and after spike removal, and in (b) the subtraction is shown.

Statistical parametric mapping was applied to statistically compare the wavelet entropy maps of the patients and healthy controls. Family-wise error corrections ( $P < 0.05$ ) were used to correct for the multiple comparison problem of many voxels. The localization of significant differences in wavelet entropy are reported in terms of MNI coordinates.

TABLE 1. Description of Various Time-Series Measures in the Literature to Quantify the Amount of Disorder/Order

Method	Quantity/measure	Description	Reference
Wavelet analysis	Wavelet entropy	Total entropy in wavelet coefficients	(15)
Fourier analysis	Spectral entropy	Entropy in power spectrum in low frequency range (10-80 mHz)	(24)
Regional homogeneity	Kendall's coefficient of concordance (KCC)	Measure of similarity of time-series in a voxel and its nearest neighbors	(25)
Hurst exponent	Fractal measure	Long-term measure of memory; $H=0.5$ indicates uncorrelated time series, 0-0.5 high long-term autocorrelation, while for 0.5-1.0 long-term switching in adjacent pairs happens	(29)
Entropy	Shannon entropy	Order/disorder in BOLD time series computed using Shannon entropy of time series	(6)



**FIGURE 5: (a)** Fourier-based power spectrum of patients and controls. There were no obvious differences observed for any of the frequency bands between patients and controls. The frequency intervals of the (wavelet) subbands are added to the graph. **(b)** Spectral energy binned according to the subband intervals of the wavelet transform. **(c)** Squared amplitudes of wavelet subbands in patients and controls. The amplitudes are used to compute the wavelet entropy. In both patients and controls the energy in wavelet subbands gradually decreases from lower to higher subbands. Patients show lower energy than controls in subbands 2–5, which makes the energy distribution across subbands more uniform (flatter spectrum) in patients, and increases the wavelet entropy. The spectral energy (in b) showed a similar trend as the wavelet energy (in c) as a function of the subband. However, differences in spectral entropy in patients and controls were not significant. Error bars are standard errors of mean.

## Results

Using the model time series, Fig. 2 gives a comparison of the Shannon entropy of the time series, wavelet entropy, and spectral entropy. It can be observed that the wavelet entropy increases relatively stronger than the Shannon entropy or spectral entropy with increasing amplitude of the nonstationary (dampened sinusoid) component in the time series. From Fig. 2a–c, the Shannon entropy increases by 2–3%, spectral entropy by 25%, and wavelet entropy by 70%.

Figure 5 shows the power spectrum (Fourier transform) and wavelet subbands of patients and controls. The power spectrum was not different between patients and controls. The energy in wavelet subbands gradually decreases from lower to

higher subbands in both patients and controls. Patients show lower energy than controls in subbands 2–5, which makes the energy distribution across subbands more uniform (flatter spectrum) in patients, and increases the wavelet entropy.

Wavelet entropy values for the whole cerebrum are listed in Table 2. In patients, for the whole cerebrum a significantly higher wavelet entropy was found compared to controls ( $P = 0.03$ ). Also, for the Rolandic strip the wavelet entropy was elevated in patients relative to controls ( $P = 0.04$ ).

Analyzing the whole cerebrum, a sensitivity of 80% and specificity of 73% was obtained using the wavelet entropy measure. The area under the curve indicates robustness of the method, as it was  $0.75 \pm 0.04$  (mean  $\pm$  standard deviation).

The wavelet entropy maps for patients with Rolandic epilepsy and healthy controls are shown in Fig. 6 and the MNI coordinates of regions where the patients' wavelet entropy is elevated are listed in Table 3. In addition to the Rolandic strip (sensorimotor cortex), the patients' wavelet entropy was elevated in a number of other brain regions, including the inferior prefrontal cortex (Broca's area), precuneus, insula, and lateral occipital cortex. No regions showed significantly lower wavelet entropy in patients relative to controls.

## Comparison With Other Time Series Measures

Table 2 also lists the results using frequency measures such as spectral entropy and other standard methods such as the Shannon entropy of time series, ReHo, and Hurst exponent. For patients, the average Hurst exponent was slightly lower and closer to 0.5 than in controls. Spectral entropy was higher and ReHo was lower for patients than controls, indicating higher randomness in the time series of patients. Most of the measures gave an indication of increased randomness of the patients' signals compared to the healthy controls. However, none of these results, other than wavelet entropy, were significant. Table 2 also shows results using measures such as fALFF, wavelet energy, and binned spectral entropy. The results using these measures were not significant.

## Discussion

In this study we presented the wavelet entropy measure to quantify temporal irregularities in BOLD time series. This method applies wavelet decomposition to the time series and determines the frequency structure of the wavelet components over various subbands. Model time series showed that the wavelet entropy measure was more sensitive to the identification of nonstationary components than conventional measures of disorder/order such as Shannon and spectral entropy. As an application, we analyzed abnormalities in the resting-state BOLD time series of children with Rolandic epilepsy. The wavelet entropy method was found to be sensitive to detect abnormal cerebral fluctuations in BOLD

**TABLE 2. Comparison of Time-Series Measures Between Children With Rolandic Epilepsy and Healthy Controls for the Whole Cerebrum and Bilateral Rolandic Strip**

Measure	Whole cerebrum			Rolandic strip		
	Patients	Controls	<i>P</i> -value	Patients	Controls	<i>P</i> -value
<i>Disorder/order measures</i>						
Wavelet entropy	1.765 ± 0.013	1.731 ± 0.011	0.03	1.760 ± 0.079	1.736 ± 0.087	0.04
Entropy of time-series	6.534 ± 0.187	6.584 ± 0.024	0.32	6.525 ± 0.258	6.575 ± 0.031	0.72
Spectral entropy	6.567 ± 0.007	6.557 ± 0.011	0.41	6.587 ± 0.011	6.576 ± 0.012	0.61
Spectral entropy (binned)	2.771 ± 0.003	2.767 ± 0.004	0.22	2.776 ± 0.003	2.772 ± 0.003	0.34
ReHo (10-80mHz)	0.420 ± 0.009	0.429 ± 0.011	0.52	0.407 ± 0.011	0.408 ± 0.012	0.81
Hurst exponent	0.795 ± 0.005	0.800 ± 0.008	0.42	0.795 ± 0.006	0.801 ± 0.009	0.76
<i>Fluctuation strength measures</i>						
fALFF	0.371 ± 0.041	0.378 ± 0.039	0.08	0.370 ± 0.005	0.371 ± 0.004	0.50
Wavelet energy	64.5 ± 1.7	64.5 ± 2.7	0.93	63.1 ± 2.0	62.7 ± 2.9	0.91

Disorder/order measure values are given for the wavelet entropy measure, spectral entropy, and other standard methods including the (Shannon) entropy of time-series, Regional Homogeneity (ReHo), and Hurst exponent. Fluctuation strength measures are the (Fourier-based) fractional amplitude of low-frequency oscillations (fALFF) and the wavelet energy. Values are represented as mean ± standard error.

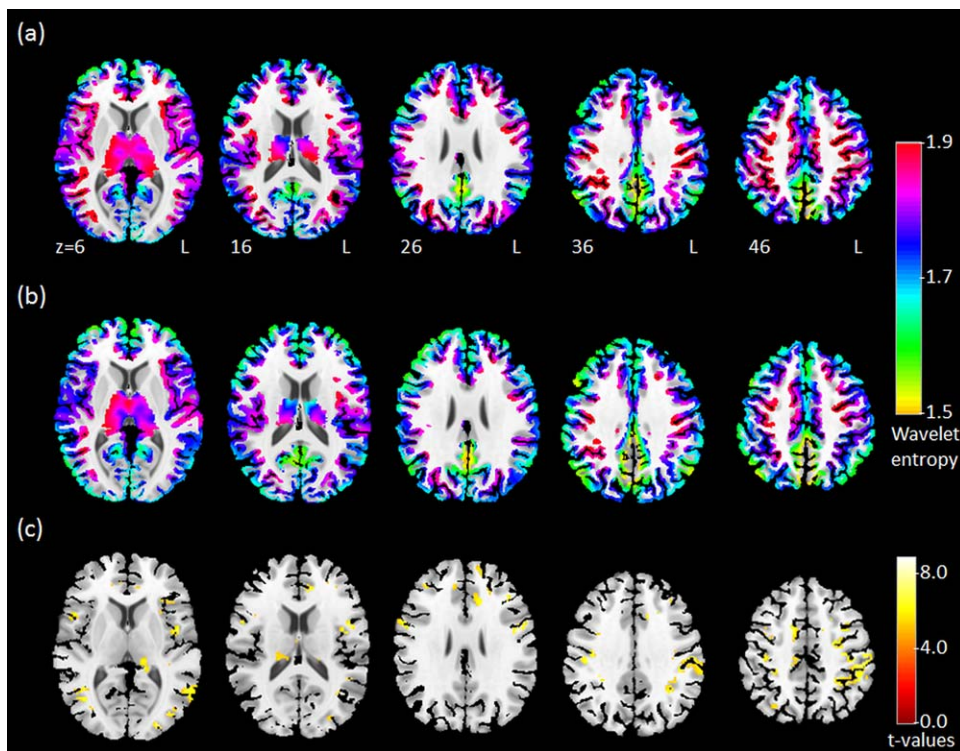


**FIGURE 6: Group averaged wavelet entropy brain maps for children with Rolandic epilepsy (a) and healthy controls (b). The entropy is only mapped on the gray matter by applying a gray matter mask on the smoothed and group averaged wavelet entropy maps. Statistical parametric mapping of the difference is depicted in (c). Wavelet entropy is significantly elevated in patients compared to controls in brain regions including the (bilateral) sensorimotor cortex, (left) inferior prefrontal (Broca's area), precuneus, insula, and lateral occipital cortex. Coordinates are in the frame of the Montreal Neurological Institute.**

**TABLE 3. Summary of Regions Where the Patients' Wavelet Entropy is Elevated.**

MNI coordinates (mm)			Maximum <i>t</i> -value	<i>P</i> -value (cluster)	Anatomical region
x	y	z			
-40	-10	-6	8.90	<0.001	Insula
-46	4	14	8.42	0.001	Inferior prefrontal
-32	-20	46	7.24	0.001	Sensorimotor
-48	0	26	8.22	0.007	Precentral (Sensorimotor)
-44	-42	38	7.64	<0.001	Sensorimotor
-18	-46	54	6.87	0.012	Precuneus
-42	-74	6	8.70	<0.001	Lateral occipital

Regions were identified by applying statistical parametric mapping to statistically compare the wavelet entropy maps of the patients and healthy controls. Coordinates are given in the standardized MNI (Montreal Neurological Institute) frame. Family-wise error corrections ( $P < 0.05$ ) were used to correct for the multiple comparison problem of many voxels.

time series and was significantly elevated in children with Rolandic epilepsy in comparison to healthy controls.

The wavelet entropy method is based on the decomposition of the time series signals into different frequency bands using Daubechies wavelet analysis. It was observed that the energy of subbands roughly decreases from lower to higher frequency subbands in patients as well as healthy controls. This indicates a variation (or structure) in pattern of information content over the frequency subbands of the BOLD time series.<sup>3</sup> The wavelet entropy measure captures this frequency structure, which makes it more appropriate to study abnormalities in the BOLD time series represented by nonstationary effects than more conventional measures. Unlike DFT or STFT, with DWT the time-frequency structure of the signal can be followed with optimal temporal resolution, which helps to represent nonstationary components in wavelet subbands. The nonstationary components are detected by the DWT of the BOLD-time series by means of the convolution with the (time shifted and scaled) mother wavelet function. Subsequently, the resulting subbands are (squared and) integrated over time to obtain the energy per subband. DWT also helps to avoid uncontrolled spectral leakage artifacts inherent in applying DFT to a nonstationary signal. The wavelet entropy method is expected to be highly suitable to detect any nonstationary abnormalities in brain signals for diseases like epilepsy.

Several studies have indicated that the amplitudes of the BOLD signal (for instance, amplitude of low-frequency fluctuations) in predefined frequency bands differed between patients with epilepsy and controls.<sup>31</sup> However, the abnormal frequency bands might vary over various types of epilepsy and also patient by patient.<sup>32</sup> This variation might also be due to dynamic nature of abnormal brain activity. In

other words, abnormalities might not consistently appear in certain (predefined) frequency bands, but may vary over time (ie, nonstationarity) across different frequency bands.<sup>33</sup> The wavelet entropy measure captures such nonstationary signal effects (or temporal variations of the frequency spectrum) by analyzing the time series by means of a wavelet transform.

Our results showed significantly elevated wavelet entropy in patients compared to healthy controls when averaged over the entire cerebrum. It was observed that a number of the patients' brain regions in particular showed elevated wavelet entropy, indicating that this is a distributed and widespread, rather than a focal, effect. These regions included the sensorimotor cortex (Rolandic strip), inferior prefrontal cortex (Broca's area, language region), and precuneus (default mode network regions). It is interesting to note that the wavelet entropy is elevated in the Rolandic strip, which is the seizure onset zone, and also in a language region, as we know that language function is often impaired in Rolandic epilepsy. Previously applied functional connectivity methods also showed significant differences between patients with Rolandic epilepsy and controls in these regions (Rolandic strip, language regions, and default mode network regions) in the literature.<sup>22,34</sup> However, it needs to be remarked that a spatial overlap (SPM) analysis, as applied in this study, only reveals brain areas that coherently over the patients show abnormalities in the time series signal, while more heterogeneously (spatially) distributed abnormalities may remain undetected.<sup>35</sup>

The spontaneous BOLD fluctuations were not found to differ between patients and controls using methods such as spectral entropy, regional homogeneity, Hurst exponent, and entropy of time series. Spectral entropy is a measure of disorder/order that is determined from the power spectrum

of the signal. Our results using this method on the BOLD time series of children with Rolandic epilepsy were not significant, likely because spectral entropy is not suitable for detecting changes in nonstationary time signals.<sup>8</sup> The method by binning spectral energy to the frequency intervals to comply with the wavelet subband frequency ranges showed a similar trend as the wavelet energy as a function of the subband. However, differences in spectral entropy in patients and controls were not significantly different. It has to be remarked that comparing the binned spectral entropy and wavelet entropy might not be accurate, because 1) the spectral energy is calculated in the frequency domain, whereas the wavelet energy is calculated in the time domain; 2) due to leakage effects, harmonic frequency ranges do not fully comply with wavelet subbands; and 3) the Fourier frequency binning deals with a frequency increment (subband width) that is larger than the actual frequency resolution for which data are averaged over time windows shorter than the full acquisition time, which likely mostly affects the slow frequency values, whereas the wavelet approach considers the full acquisition duration. Most important, the wavelet entropy measure appears more capable of detecting changes in a nonstationary signals due to the localization characteristics of the wavelet transform, which makes it more appropriate to detect abnormal changes in dynamic brain signals, with changing frequencies over time, in diseases like epilepsy.<sup>3,33</sup>

Also, the regional homogeneity measure could reveal abnormalities in the disorder/order of the time series of the Rolandic epilepsy children. The ReHo method assumes that within a functional cluster of neighboring voxels, the hemodynamic characteristics of each voxel will be highly similar (or synchronous).<sup>36</sup> However, this measure may suffer from a partial volume-averaging ( $T_2^*$  blurring) effect at the millimeter scale among adjacent areas in the gray matter. Due to the blurring of areas on  $T_2^*$  images, the ReHo measure that relies on the variation of intensities among adjacent voxels might be attenuated. Thus, the ReHo measure became insensitive to local variations and has reduced the differences in adjacent voxels in the BOLD image.<sup>37</sup>

The assumption of changes in self-similarity, which is required for the Hurst exponent, was not observed in patients with Rolandic epilepsy. As the Hurst exponent has not previously been used in epilepsy, comparison with other studies is not possible yet. The value of the Hurst exponent for patients was closer to 0.5 than in controls, indicating more strongly uncorrelated, thus random, signals. All the above measures on disorder/order hinted at stronger, although statistically insignificant, disorder in the time signal for the patients with Rolandic epilepsy. However, only the wavelet entropy measure appeared sufficiently sensitive to capture and quantify these temporal irregularities. Entropy of time series did also not reveal significant differences

between patients and controls. This measure has also not been used on fMRI and EEG time series in the literature. The results using this measure hint that more complex measures of time series are required for measuring homogeneity/heterogeneity in BOLD time series data.

Independent of the amplitude (or energy) of the signal fluctuations, the wavelet entropy measure provides new information on the frequency structure of brain signals in comparison to Fourier-based or other methods. An additional advantage of the wavelet entropy measure is that it is parameter-free and the computation time of wavelet entropy is relatively shorter than other spectral methods since the algorithm uses fast wavelet transform in a multiresolution framework.<sup>38</sup>

The children with Rolandic epilepsy showed more irregular nonstationary BOLD signals in many brain regions in comparison to healthy controls. It seems straightforward to relate these dynamic regularities to possible epileptiform activity of the epileptic brain. Epileptic brain activity is expectedly of very high frequency compared to the measured frequency range and it remains unknown how this translates into BOLD fluctuations. These assumptions need further investigations where, for instance, EEG activity is spatiotemporally linked to the BOLD signal by integrated simultaneous fMRI-EEG measurements. Whether these children experienced (subclinical) epileptiform activity during the MRI scan is unlikely or highly uncertain. For now, it remains unknown whether the observed abnormalities in the frequency structure of the BOLD signal is directly due to epileptiform activity or merely reflects a more disordered resting-state brain signal.

The current study demonstrates the application of a novel disorder/order measure for characterizing irregularities in dynamic brain signals of children with a relevant brain disease for which time series abnormalities may be expected. However, there are also a number of considerations that deserve future attention, including the above-mentioned validation with simultaneously recorded fMRI-EEG signals. The current study design is retrospective, and not prospective, which is, however, generally considered sufficient for diagnostic research. Furthermore, the selection of the wavelet filter is rather critical to decompose the signal into different frequency subbands. In this study we used a Daubechies wavelet filter, which gave us satisfactory results on the Rolandic epilepsy patients. As a scope of future work, a new set of wavelet filters could be designed that can closely represent the BOLD signal from healthy controls. The filter design requires a huge amount of data from healthy controls that can help in determining the most appropriate shape for the function.<sup>39</sup>

In conclusion, this study presents the wavelet entropy measure for quantifying irregularities in BOLD time series from the brain. The wavelet-based measure gave new

information about the loss of frequency structure of irregular brain signals and appeared more sensitive than Fourier-based spectral entropy and other standard methods. The observation of elevated wavelet entropy obtained in children with Rolandic epilepsy are encouraging and, in the future, the proposed technique could be further expanded to different epilepsy syndromes and other brain disorders.

## References

- Ponce-Alvarez A, Deco G, Hagmann P, Romani GL, Mantini D, Corbetta M. Resting-state temporal synchronization networks emerge from connectivity topology and heterogeneity. *PLoS Comput Biol* 2015;11:1–23.
- Liu CY, Krishnan AP, Yan L, et al. Complexity and synchronicity of resting state blood oxygenation level-dependent (BOLD) functional MRI in normal aging and cognitive decline. *J Magn Reson Imaging* 2013;38:36–45.
- Smith RX, Jann K, Ances B, Wang DJJ. Wavelet-based regularity analysis reveals recurrent spatiotemporal behavior in resting-state fMRI. *Hum Brain Mapp* 2015;36:3603–3620.
- Tobia MJ, Iacovella V, Hasson U. Multiple sensitivity profiles to diversity and transition structure in non-stationary input. *NeuroImage* 2012;60:991–1005.
- Smith RX, Yan L, Wang DJJ. Multiple time scale complexity analysis of resting state fMRI. *Brain Imaging Behav* 2013;8:284–291.
- de Araujo DB, Tedeschi W, Santos AC, Elias J Jr, Neves UPC, Baffa O. Shannon entropy applied to the analysis of event-related fMRI time series. *NeuroImage* 2003;20:311–317.
- Powell GE, Percival IC. A spectral entropy method for distinguishing regular and irregular motion of hamiltonian systems. *J Phys A Math Gen* 1979;12:2053–2071.
- Inouye T, Shinosaki K, Iyama A, Matsumoto Y. Localization of activated areas and directional EEG patterns during mental arithmetic. *Electroencephalogr Clin Neurophysiol* 1993;86:224–230.
- Leonardi N, Van De Ville D. On spurious and real fluctuations of dynamic functional connectivity during rest. *NeuroImage* 2015;104:430–436.
- Mallat S. *A wavelet tour of signal processing*. San Diego: Academic Press; 1999.
- Rosso OA. Entropy changes in brain function. *Int J Psychophysiol* 2007;64:75–80.
- Koutroumanidis M. Panayiotopoulos syndrome: an important electro-clinical example of benign childhood system epilepsy. *Epilepsia* 2007;48:1044–1053.
- Panayiotopoulos CP. *Benign childhood partial seizures and related epileptic syndromes*. London: John Libbey & Co.; 1999.
- Mooij AH, Frauscher B, Amiri M, Otte WM, Gotman J. Differentiating epileptic from non-epileptic high frequency intracerebral EEG signals with measures of wavelet entropy. *Clin Neurophysiol* 2016;127:3529–3536.
- Rosso OA, Blanco S, Yordanova J, et al. Wavelet entropy: a new tool for analysis of short duration brain electrical signals. *J Neurosci Methods* 2001;105:65–75.
- Daubechies I. *Ten lectures on wavelets*. SIAM, Philadelphia: CBMS-NSF Lecture Notes; 1992.
- Mallat SG. A theory for multiresolution signal decomposition: the wavelet representation. *IEEE Trans Pattern Anal Mach Intell* 1989;11:674–693.
- Overvliet G, Besseling R, Kruijs Svd, et al. Clinical evaluation of language fundamentals in Rolandic epilepsy, an assessment with CELF-4. *Eur J Paediatr Neurol* 2013;17:390–396.
- Zou Q-H, Zhu C-Z, Yang Y, et al. An improved approach to detection of amplitude of low-frequency fluctuation (ALFF) for resting-state fMRI: Fractional ALFF. *J Neurosci Methods* 2008;172:137–141.
- Windischberger C, Langenberger H, Sycha T, et al. On the origin of respiratory artifacts in BOLD-EPI of the human brain. *Magn Reson Imaging* 2002;20:575–582.
- Fischl B, Salat DH, Kouwe AJWvd, Makris N, Ségonne F, Dale AM. Sequence-independent segmentation of magnetic resonance images. *NeuroImage* 2004;23:569–584.
- Besseling RMH, Overvliet GM, Jansen JFA, et al. Aberrant functional connectivity between motor and language networks in rolandic epilepsy. *Epilepsy Res* 2013;107:253–262.
- Patel AX, Kundu P, Rubinov M, et al. A wavelet method for modeling and despiking motion artifacts from resting-state fMRI time series. *NeuroImage* 2014;95:287–304.
- Jantti V, Alahuhta S, Barnard J, Sleight JW. Spectral entropy — what has it to do with anaesthesia, and the EEG. *B J Anaesth* 2004;93:150–152.
- Zang Y, Jiang T, Lu Y, He Y, Tian L. Regional homogeneity approach to fMRI data analysis. *NeuroImage* 2004;22:394–400.
- Baumgartner R, Somorjai R, Summers R, Richter W. Assessment of cluster homogeneity in fMRI data using Kendall's coefficient of concordance. *Magn Reson Imaging* 1999;17:1525–1532.
- Cheng WL, Qian YZ, Zhang ZQ. fMRI study of temporal lobe epilepsy using ReHo analysis. *Acta Biophys Sin* 2008;24:460–464.
- Qiao P-F, Gao P-Y, Dai J-P, Niu G-M. Research progress on resting state fMRI of epilepsy. *Brain Dev* 2012;34:8–12.
- Carbone A, Castelli G, Stanley HE. Time-dependent Hurst exponent in financial time series. *Physica A Stat Mech Appl* 2004;344:267–271.
- Zeng L, Liu Q, Xiao H, Chen H. Support vector machine on functional MRI, advances in cognitive neurodynamics. *ICCN* 2007;4:915–918.
- Wang Z, Zhang Z, Liao W, et al. Frequency-dependent amplitude alterations of resting-state spontaneous fluctuations in idiopathic generalized epilepsy. *Epilepsy Res* 2014;108:853–860.
- Li C, Liu C, Yin X, et al. Frequency-dependent changes in the amplitude of low-frequency fluctuations in subcortical ischemic vascular disease (SIVD): A resting-state fMRI study. *Behav Brain Res* 2014;274:205–210.
- Milton JG. Epilepsy as a dynamic disease: A tutorial of the past with an eye to the future. *Epilepsy Behav* 2010;18:33–44.
- Oser N, Hubacher M, Specht K, Datta AN, Weber P, Penner I-K. Default mode network alterations during language task performance in children with benign epilepsy with centrotemporal spikes (BECTS). *Epilepsy Behav* 2014;33:12–17.
- Gupta L, Besseling RMH, Overvliet GM, et al. Spatial heterogeneity analysis of brain activation in fMRI. *NeuroImage Clin* 2014;5:266–276.
- Katanoda K, Matsuda Y, Sugishita M. A spatial-temporal regression model for the analysis of functional MRI data. *NeuroImage* 2002;17:1415–1428.
- Kang Y, Choi SH, Kim Y-J, et al. Gliomas: Histogram analysis of apparent diffusion coefficient maps with standard- or high-b-value diffusion-weighted MR imaging—correlation with tumor grade. *Radiology* 2011;261:882–890.
- Uytterhoeven G, Van Wulpen F, Jansen M, Roose D, Bultheel A. *WALL: a software library for image processing using integer wavelet transforms*. San Diego, CA: SPIE digital library; Vol 3338; 1998 p. 1490–1501.
- Vetterli M, Herley C. Wavelets and filter banks: theory and design. *IEEE Trans Signal Process* 1992;40:2207–2232.